International Journal of Chemical, Materials and Biomolecular Sciences
ISSN: 2415-6620
Vol:6, No:11, 2012

A Highly Efficient Process Applying Sige Film to Generate Quasi-Beehive Si Nanostructure for the Growth of Platinum Nanopillars with High Emission Property for the Applications of X-Ray Tube

Pin-Hsu Kao, Wen-Shou Tseng, Hung-Ming Tai, Yuan-Ming Chang, and Jenh-Yih Juang

***Abstract*—**We report a lithography-free approach to fabricate the biomimetics, quasi-beehive Si nanostructures (QBSNs), on Si-substrates. The self-assembled SiGe nanoislands via the strain induced surface roughening (Asaro-Tiller-Grinfeld instability) during in-situ annealing play a key role as patterned sacrifice regions for subsequent reactive ion etching (RIE) process performed for fabricating quasi-beehive nanostructures on Si-substrates. As the measurements of field emission, the bare QBSNs show poor field emission performance, resulted from the existence of the native oxide layer which forms an insurmountable barrier for electron emission. In order to dramatically improve the field emission characteristics, the platinum nanopillars (Pt-NPs) were deposited on QBSNs to form Pt-NPs/QBSNs heterostructures. The turn-on field of Pt-NPs/QBSNs is as low as 2.29 V/μm (corresponding current density of 1 μA/cm2), and the field enhancement factor (β-value) is significantly increased to 6067. More importantly, the uniform and continuous electrons excite light emission, due to the surrounding filed emitters from Pt-NPs/QBSNs, can be easily obtained. This approach does not require an expensive photolithographic process and possesses great potential for applications.

***Keywords*—**Biomimetics, quasi-beehive Si, SiGe nanoislands, platinum nanopillars, field emission.

I. Introduction

DUE to attractive properties—non-toxicity, stability at room temperature, and high natural abundance [1], silicon (Si) is the most dominated semiconductor material for industrial applications. Superior to other nanostructures in their compatibility with Si-based manufacturing processes, Si-nanostructures are highly promising for integration with Si semiconductor fabrication to form active electron nano-micro devices. Therefore, Si-nanostructures are widely used in fabricating high-performance optoelectronic devices for industrial [2-7]. Among the vacuum optoelectronic devices, field emitters are of great technological importance to field emission displays applications. Considerable methods, thus, to fabricate single-crystalline Si nanoemitters have been developed. For instance, Yang *et al.* [8] applied selective chemical-etching technique to form SiC porous nanowires; The SnO_2-capped Si nanowires, presented by Chi *et al.* [9], were synthesized in a horizontal tube furnace via chemical vapor deposition (CVD). To fully realize the application potential, the field emitters for fabricating flat-panel display are required continuous electron emission after applying voltage. The screen quality of flat-panel display is extremely dependent on uniform and continuous electron emission. The most reported studies, unfortunately, do not meet these requirements. On the other hand, it has been demonstrated that electrons are more easily emitted from nanostructures with sharp tips. This has inspired researchers to make significant efforts to decrease the tip size and increase the number of active emitting centers.

In this work, the biomimetics nanostructure, quasi-beehive Si nanostructures (QBSNs), have the important feature of continuous electron emission, are presented. The QBSNs were fabricated by using a novel approach, which does not need any lithography process. The SiGe thin films deposited by ultrahigh vacuum chemical vapor deposition (UHVCVD) form self-assembled nanoislands via the strain induced surface roughening during thermal annealing, which, in turn, serve as patterned sacrifice regions for subsequent reactive ion etching (RIE) process carried out for fabricating QBSNs on Si-substrates. To further increase the electronic properties, on the other hand, the platinum nanopillars (Pt-NPs) were deposited on QBSNs to form Pt-NPs/QBSNs heterostructures. It is important to note that the tops of Pt-NPs possess multiple tips whose mean radius are only 1~3 nm. These nanotips on Pt-NPs are useful to promote the field emission performance for Pt-NPs/QBSNs. The Pt-NPs/QBSNs have the advanced advantages, such as continuous electronic emission pattern, low turn-on field and high enhancement factor, which make them extraordinary nanoemitters for flat-panel display

P. H. Kao is with the Center for Measurement Standards of Industrial Technology Research Institute. Hsinchu 300, Taiwan (corresponding author to provide phone: 886-3-5743879; fax: 886-3-5722383; e-mail: PHKao@itri.org.tw).

W. S Tseng is with Center for Measurement Standards of Industrial Technology Research Institute, Hsinchu 300, Taiwan (e-mail: itri990210@itri.org.tw).

H. M. Tai is with Center for Measurement Standards of Industrial Technology Research Institute, Hsinchu 300, Taiwan(e-mail: HMTai@itri.org.tw

Y.-M. Chang is with the Department of Electrophysics, National Chiao Tung University, Hsinchu 300, Taiwan. (e-mail: ymchang7@gmail.com).

J.-Y. Juang is with the the Department of Electrophysics, National Chiao Tung University, Hsinchu 300, Taiwan. (e-mail: jyjuang@g2.nctu.edu.tw).

II. Experiments

SiGe epitaxial thin films were grown onto 6-inch p-type Si (100) in an UHVCVD system (ANELVA SRE-612). The Si wafers had undergone standard cleaning according to the guidelines of the Radio Corporation of America (RCA) [10]; they were dipped in dilute hydrofluoric acid to passivate their surfaces. As a result, when the wafers were transported through air and introduced into the loadlock chamber of the UHVCVD system, their surfaces remained cleaned. As soon as the system temperature was increased to 550 °C, and the deposition chamber was pumped to 1.2×10^{-9} Torr using a turbo molecular pump, the wafers were transferred directly to the deposition chamber from the loadlock chamber. The inlet gases were a mixture of Si_2H_4 at a flow rate of 1 sccm and GeH_4 at a flow rate of 7 sccm. Following the growth of the thin film, *in situ* thermal annealing was performed at 900 °C for 30 min in the UHVCVD chamber.

Cross-sectional TEM images of thin films were obtained using a transmission electron microscope (JEOL JEM-2010F) with an operating voltage of 200 kV; the compositions of thin films were verified using energy-dispersive X-ray spectroscopy (EDS). HRXRD (PANalytical X'Pert Pro) with Cu Kα radiation (λ = 0.154 nm) was applied to determine the phase formation and the crystallographic structure of all samples. A hybrid monochromator and a triple-axis x-ray diffractometer were adopted in a rocking curve to observe the structural features of the SiGe thin films. Tapping-mode AFM (Veeco Dimension 5000) was used to image the surface morphologies of the SiGe thin films at a constant frequency of 1.0 Hz. The Pt-NPs were deposited by using rf-sputter (JEOL JFC-1600) for 180 seconds. Moreover, the samples were loaded into a vacuum chamber (5×10^{-6} torr) to measure the field emission current. The phosphor (P_{22}) which was applied in the cathode-ray tube displays was deposited on a transparent conductive material (indium-tin-oxide), to be an anode electrode in the vacuum system and the cathode voltage was applied to the Si-substrates.

III. Results and Discussion

Figure 1 shows the typical top-view image observed by FESEM for SiGe films annealed at 900 °C for 30 min. It is clear that the high temperature annealing-induced surface roughening has led the formation of the self-organized SiGe islands along the (100) and (010) directions. The cross-sectional image of SiGe islands on Si-substrate is observed by TEM displayed in the inset of Figure 1 further indicates that in the vicinity of the interface between the SiGe islands and Si-substrate remains essentially free of relaxation dislocations during the annealing process. The further detailed mechanism for the formation of SiGe islands was described in Ref. [10, 11].

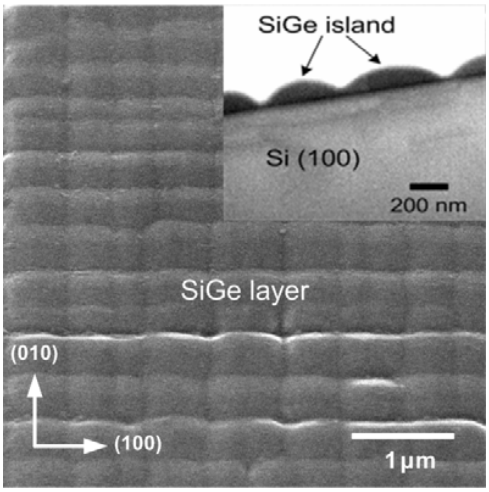

Fig. 1 SEM observation the surface morphological image of SiGe thin film at an annealing temperature of 900 °C. The inset is the TEM image of SiGe nanoislands on Si-substrate

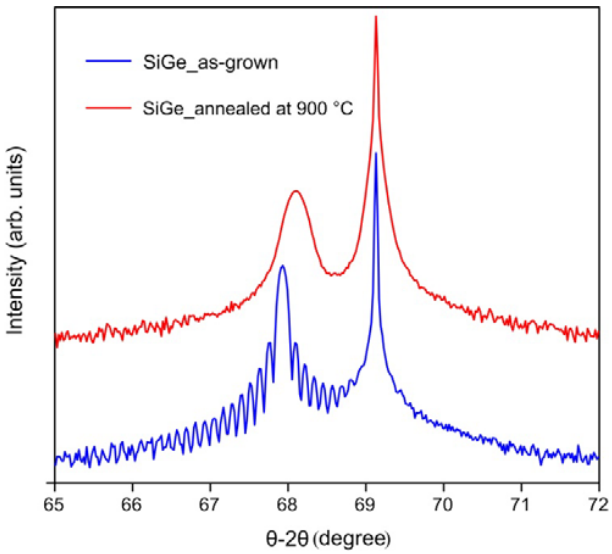

Fig. 2 The XRD spectra of (a) the as-grown SiGe thin film and, (b) the annealed SiGe thin film at 900 °C for 30 min

We used HRXRD analysis to characterize the crystallographic structure of the SiGe thin film. Figure 2 displays the XRD curves of the (004) reflections from as-grown SiGe and SiGe thin film that had been annealed at annealing temperature of 900 °C, respectively. The curve of the as-grown film had two sharp peaks: one at 69.12° was from the Si-substrate and the other at 67.92° represented the SiGe film. Additionally, the as-grown SiGe shows the well-defined thickness fringes from the interface, and the oscillation properties indicate high epitaxial growth of SiGe on Si-substrate. The result is good agreement with the HRTEM observation revealed in Figure 1(b). On the other hand, the SiGe signal of the film that had been annealed at 900 °C shifted the SiGe peak further to 68.10°. This change in the SiGe peak

position proves that the film underwent strain relaxation during thermal annealing [12]. Moreover, the oscillation for the SiGe sample disappeared following the thermal annealing as a result of the interface broadening due to the interdiffusion between the thin film and the Si-substrate. That is to say, the interface changed during thermal annealing at high temperature of 900 °C [10, 13].

Being inspired by defective SiGe thin film presented in Figure 1, we have further tried to use the annealed sample as the template for creating the QBSNs [11]. In order to enhance the electronic performance, the Pt element was deposited on QBSNs to form Pt-NPs/QBSNs heterostructures.

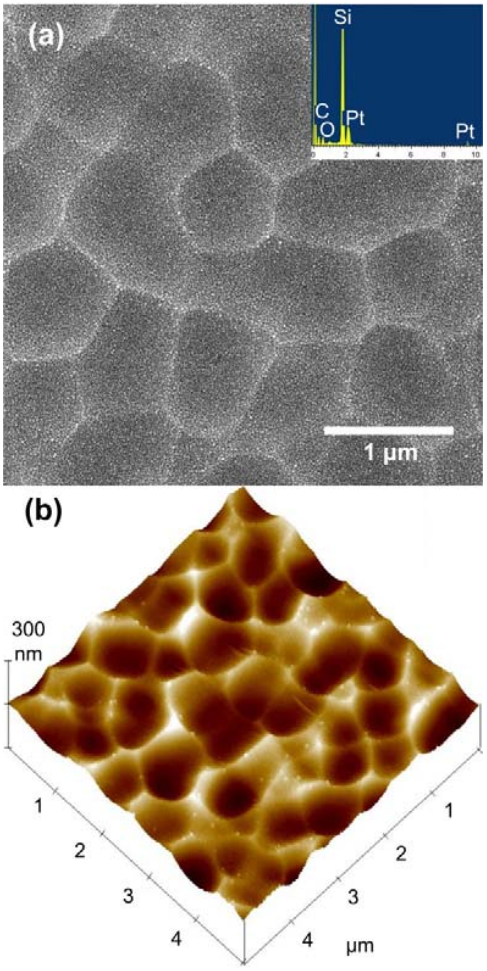

Fig. 3 The (a) SEM and (b) AFM image of Pt-NPs on QBSNs.

Figure 3(a) and (b) show the typical SEM and AFM image of presented Pt-NPs/QBSNs. Figure 3 evidently displays that the QBSNs, biomimetics, is consisting of nano-cavities and edges. It is important to note that the continuous edges from QBSNs are clear to form surrounding emitters for latter field emission applications. The EDS spectrum displayed in the inset in Figure 3(a) for the Pt-NPs/QBSNs sample does reveal the existence of Pt on QBSNs.

To further investigate the crystalline structure of the Pt obtained by sputtering process, the grazing incidence XRD was carried out. Figure 4 shows the XRD curve obtained for the Pt films deposited on QBSNs. It is evident that for Pt deposited at room temperature there are three distinctive diffraction peaks corresponding to(111), (200) and (220) crystallographic orientations. The results suggest that the Pt deposited on the QBSNs at room temperature, while remains largely polycrystalline, is of good crystalline quality. The inset in displayed in Figure 4 does reveal the existence of Pt-NPs on QBSNs.

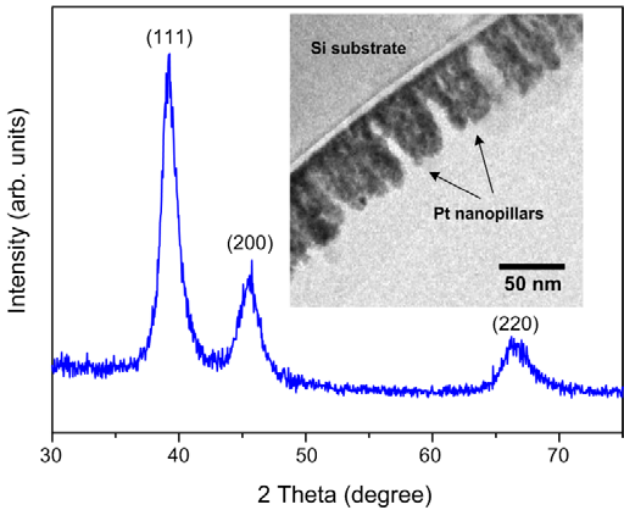

Fig. 4 The XRD spectrum of Pt-NPs on QBSNs. The inset is the high-magnification TEM image of Pt-NPs/QBSNs

In order to investigate the structural properties of Pt-NPs/QBSNs in detailed, the observations of TEM were carried out. Figure 5(a) displays the cross-sectional TEM image of Pt-NPs on QBSNs. According to this picture, the QBSNs possess hill-like shape in their cross-sectional view. The characteristic is a very important to enhance the electronic performance for QBSNs. It is well known that the structure, which has large curvature, can give rise to the collection of electrons. The hill-like shape of QBSNs, thus, can contribute to promote the electrons collection preliminary. Additionally, the dense Pt-NPs grown on the surface of QBSNs can be clearly observed in Figure 5(a). The inset in Figure 5(a) shows the electron diffraction pattern obtained from a selected area of Pt-NPs. The bright rings with occasional bright spots are due to the presence of polycrystalline. The result is good agreement of the XRD data revealed in Figure 4. Unfortunately, this picture only provides limited information of Pt-NPs/QBSNs. Figure 5(b) displays the HRTEM image of Pt-NPs/QBSNs. It is important to note that the space between separated pillars can be found clearly. Figure 5(b) shows HRTEM image of the end for single Pt-NP, displaying the presence of multiple tips, as indicated by white arrows. These nanosize tips are connected with the pillar body. It is interest to note that the mean radius of these tips is only of 1~3 nm, resulted in attracting considerable

electrons. The structural feature might improve the field emission performance of Pt-NPs/QBSNs [14]. Figure 5(c) exhibits the HRTEM image of Pt element, where the lattice spacing is determined as 0.19 nm identifying the (202) plane. Moreover, the thickness of native oxide layer mentioned above is about 3.5 nm, as shown in Figure 5(d).

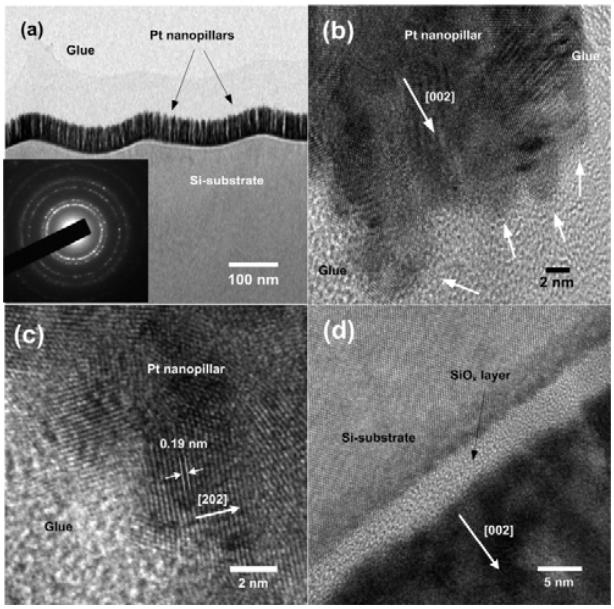

Fig. 5 The (a) TEM image of Pt-NPs on QBSNs, and the inset is the electron diffraction pattern of a region of the Pt-NPs; (b) and (c) HRTEM image of the end of individual Pt-NP; and (d) the HRTEM images of interface of Pt/QBSNs

To understand the electronic property for these biomimetics nanostructures, the measurements of field emission were carried out. Figure 6 shows the emission current density versus applied electrical field (*J-E*) curves for the prepared samples (QBSNs and Pt-NPs/QBSNs). The electric field is an average value, which was calculated from the ratio of the applied voltage to cathode–anode separation. Both the prepared samples reveal steady field emission properties at measuring distance (200 µm) between the electrodes. The emission current was measured by applying a voltage increasing from 0 to 800 V. To fully realize the application potential, decreasing the turn-on field and increasing enhancement factor for nanoemitters are thus urgently required. The bare QBSNs, unfortunately, it is evident from Figure 6 that, only diminishingly small field emission current was detected up the maximum applied field (4 V/µm) of the current setup. This is presumably due to the existence of the native oxide layer (as shown in Figure 5(d)) which forms an insurmountable barrier for electron emission. In an attempt to dramatically improve the field emission characteristics, thus, Pt-NPs were deposited on QBSNs to form Pt-NPs/QBSNs heterostructures. As can be seen from the *J-E* plot in Figure 6

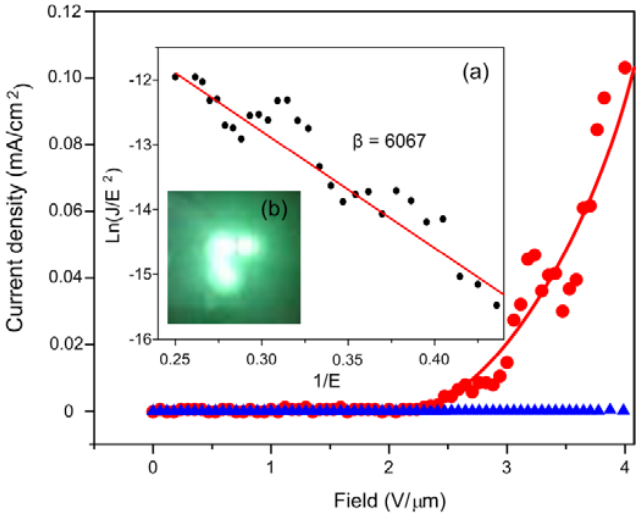

Fig. 6 Field emission *J-E* curves from the QBSNs and Pt-NPs/QBSNs at working distance of 200 µm over an effective emitting area of 1×1 cm^2. The insets (a) and (b) show the corresponding Fowler–Nordheim plot [ln (J/E^2) vs (1/E)] and electronic emission pattern from Pt-NPs/QBSNs at 4 V/µm, respectively

the turn-on threshold field, for Pt/QBSNs, is as low as 2.29 V/µm at a current density of 1 µA/cm^2, which is lower than previously measured nanostructures [15-19]. The emitted current density is around 0.1 mA/cm^2 at a bias field of 4 V/µm. In order to understand the emission behavior, the *J-E* results are analyzed by the Fowler-Nordheim (F-N) equation [20, 21]:

$$J = \frac{A\beta^2 E^2}{\phi}\exp\left(-\frac{B\phi^{3/2}}{\beta E}\right) \quad (1)$$

where J is the current density (A/m^2), E is the applied field (V/µm), ϕ is the work function (eV), β is the field enhancement factor, A and B are constants with $A = 1.56\times10^{-10}$ (A·eV/V^2) and $B = 6.83\times10^3$ (V/µm·$eV^{3/2}$), respectively. By plotting ln (J/E^2) against 1/E, a straight line was obtained for the Pt-NPs/QBSNs, as shown in the inset in Figure 6. The quasi-linear behavior of the plot reveals that these heterostructures feature field-emission behavior that follows the F-N description well. The inset (b) in Figure 6 exhibits the electrons excites light emission from phosphor screen at 4 V/µm. It's important to note that, as shown in inset (b) in Figure 6, the electrons excite light emission is a uniform and continuous pattern due to the Pt-NPs/QBSNs possess surrounding field emitters (as shown in Figure 3). By plotting ln (J/E^2) against 1/E, a nearly straight line was obtained for the Pt-NPs/QBSNs. The field enhancement factor β was calculated from the slope of the F–N plot [22]:

$$\beta = -6.83\times10^3\times\phi^{3/2} / slope \quad (2)$$

By assuming the work function of $\phi = 5.65$ eV for Pt [23], the β value of 6067 was obtained. This β value is much larger than most field emitters reported [24]. The Pt-NPs/QBSNs possess the important advantages, for instance, the indispensable advantages, for instance, continuous electronic emission pattern, low turn-on field, and high enhancement factor. These characteristics are extremely important to fabricate high performance flat-panel display for industrial applications.

If you are using *Word,* use either the Microsoft Equation Editor or the *MathType* add-on (http://www.mathtype.com) for equations in your paper (Insert | Object | Create New | Microsoft Equation *or* MathType Equation). "Float over text" should *not* be selected.

IV. Conclusion

We have demonstrated that it is possible to fabricate QBSNs on Si-substrate by simply combining the thermal annealing and RIE processes on the SiGe layers grown on Si-substrate. Via the QBSNs were decorated by Pt-NPs, the Pt-NPs/ QBSNs could be obtained with good field emission performance, such as typically turn-on field as small as 2.29 V/μm, high enhancement factor of 6067 and, the most important characteristics, continuous and uniform electronic emission pattern, are attributed to surrounding field emitters. The present study, thus, has evidently provided significant potentials for various field-emission-derived applications.

Acknowledgment

This work was partially supported by the National Science Council of Taiwan, under Grant No.: NSC 100-2811-M-009-037. Prof. J.-Y. Juang is supported in part by the National Science Council of Taiwan and the MOE-ATP program operated at NCTU. The authors would like to thank Dr. Yu-Hwa Shih, Prof. Hsin-Yi Lee (NSRRC and NCTU), Porf. Chih- Ming Lin (NHUE) for their useful discussions.

References

[1] A. Shalav, B. S. Richards, and M. A. Green, *Sol. Energ. Mat. Sol. C.* 91 (2007) 829-842.
[2] B. Tian, X. Zheng, T. J. Kempa, Y. Fang, N. Yu, G. Yu, J. Huang and C. M. Lieber, *Nature* 449 (2007) 885-890.
[3] C. K. Chan, H. Peng, G. Liu, K. Mcilerath, X. F. Zhang, R. A. Huggins and Y. Cui, *Nat. Nanotech.* 3 (2008) 31-35.
[4] Y. L. Bunimovich, Y. S. Shin, W.-S. Yeo, M. Amori, G. Kwong, and J. R. Heath, *J. Am. Chem. Soc.* 128 (2006) 16323-16331.
[5] Z. Li, Y. Chen, X. Li, T. I. Kamins, K. Nauka, and R. S. Williams, *Nano Lett.* 4 (2004) 245-247.
[6] C. T. Black, *Appl. Phys. Lett.* 87 (2005) 163116-1-3.
[7] Y. Cui, Z. Zhong, D. Wang, W. U. Wang, and C. M. Lieber, *Nano Lett.* 3 (2003) 149-152.
[8] Y. Yang, G. Meng, X. Liu, L. Zhang, Z. Hu, C. He, and Y. Hu, *J. Phys. Chem. C* 112 (2008) 20126–20130.
[9] H. Chi, H.-C. Zhu, H.-J. Xu, X.-D. Shan, Z.-M. Liao, and D.-P. Yu, *J. Phys. Chem. C* 113 (2009) 6450–6453.
[10] Y.-M. Chang, C.-L. Dai, T.-C. Cheng, C.-W. Hsu, *Thin Solid Films* 518 (2010) 3782–3785.
[11] Y.-M. Chang, S.-R. Jian and J.-Y. Juang, *Nanoscale Res. Lett.* 5 (2010) 1456–1463.
[12] S. Zheng, M. Mori, T. Tambo, C. Tatsuyama, *J. Mater. Sci.* 42 (2007) 5312-5317.
[13] S. Zheng, M. Kawashima, M. Mori, T. Tambo, C. Tatsuyama, *Thin Solid Films* 508 (2006) 156-159.
[14] Y. B. Li, Y. Bando, and D. Golberg, *Appl. Phys. Lett.* 84 (2004) 3603-3605.
[15] S. K. Marathe,P. M. Koinkar, S. S. Ashtaputre, M. A. More, S. W. Gosavi,D. S. Joag, and S. K. Kulkarni, Nanotechnology *17* (2006) 1932-1936.
[16] X. Wang, J. Zhou, C. Lao, J. Song, N. Xu, and Z. L. Wang, *Adv. Mater.* 19 (2007) 1627–1631.
[17] B. Cao, X. Teng, S. H. Heo, Y. Li, S. O. Cho, G. Li, and W. Cai, *J. Phys. Chem. C* 111 (2007) 2470-2476.
[18] Y.-K. Tseng, C.-J. Huang, H.-M. Cheng, I-N. Lin, K.-S. Liu, and I-C. Chen, *Adv. Funct. Mater.* 13 (2003) 811-814.
[19] R. T. R. Kumar, E. McGlynn, C. McLoughlin, S. Chakrabarti, R. CSmith, J. D. Carey, J. P. Mosnier, and M. O. Henry, *Nanotechnology* 18 (2007) 215704-215709.
[20] Y.-M. Chang, M.-C. Liu, P.-H. Kao, C.-M. Lin, H.-Y. Lee and J.-Y. Juang, *ACS Appl. Mater. Interfaces* 4 (2012) 1411-1416.
[21] Y.-M. Chang, J.-M. Huang, C.-M. Lin, H.-Y.Lee, S.-Y. Chen, and J.-Y.Juang, *J. Phys. Chem. C* 116 (2012) 8332-8337.
[22] V. S. Kale, R. R. Prabhakar, S. S. Pramana, M. Rao, C.-H. Sow, K. B. Jinesh, and S. G. Mhaisalkar, *Phys. Chem. Chem. Phys.* 14 (2012) 4614-4619.
[23] Y. Liu, L. Liao, J. Li, and C. Pan, *J. Phys. Chem. C* 111 (2007) 5050-5056.
[24] Y.-F. Tzeng, H.-C. Wu, P.-S. Sheng, N.-H. Tai, H. T. Chiu, C. Y. Lee, I-N. Lin, *ACS Appl. Mater. Interfaces* 2 (2010) 331-334.

Pin-Hsu Kao was born in New Taipei City, Taiwan in 1981. He received his MS and Ph.D. degree in Mechanical Engineering from the University of National Chung Hsing, Taiwan in 2005 and 2010. He is currently doing research job in Center for Measurement Standards of Industrial Technology Research Institute, Taiwan. His mainly research field is in MEMS, semiconductor and thin film process.

Wen-Shou Tseng was born in Chang-Hua Hsien, Taiwan, in 1968. He received the MSc degree in Materials Science Centre from the University of Manchester, UK, in 2002 and the Ph.D. degree in the department of Materials Science and Engineering at National Chiao-Tung University at the end of June 2009. He is currently doing research job in Center for measurement Standards of Industrial Technology Research Institute, Taiwan.

Hung-Ming Tai received his Ph.D. in the Department of Power Mechanical Engineering from National Tsing Hua University Taiwan in 1999. In 1999, he joined the Instrumentation and Sensor Development Division in Center for Measurement of ITRI, where he has worked on scanning probe microscopy, fiber sensors, and automatic optical inspection. Dr. Tai is a member of Chinese Institute of Engineers.

Yuan-Ming Chang received his MS and Ph.D. degree in Mechanical engineering from National Chung Hsing University, Taiwan, in 2004 and 2009. He is currently a post-doctor at the Department of Electrophysics, National Chiao Tung University. His research interests are nanotechnology and thin film materials.

Jenh-Yih Juang received his MS degree in Materials Science and engineering from National Tsing Hua University, Taiwan, in 1981 and his Ph.D. degree in Materials Science and engineering from Massachusetts Institute of Technology, United States of America, in 1989. He is currently a professor at the Department of Electrophysics, National Chiao Tung University, Taiwan. His research interests are superconductivity, nanotechnology, solid state physics and magnetic.